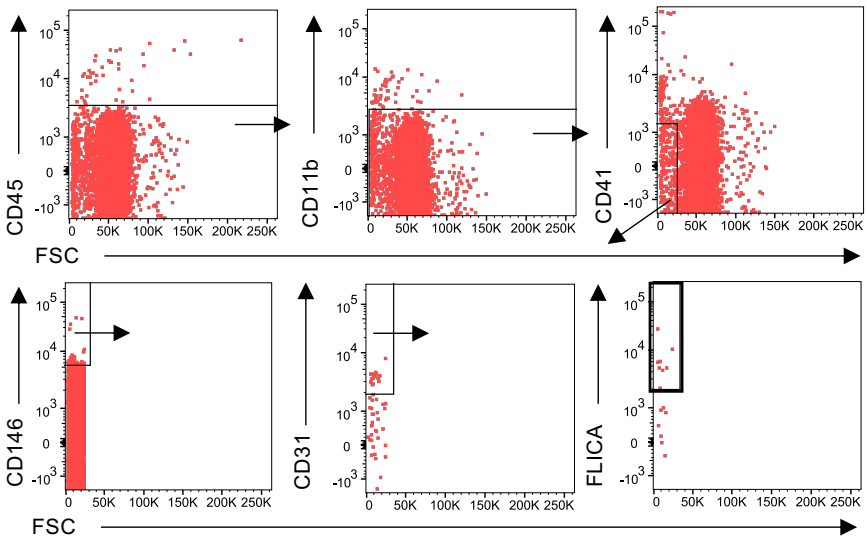

Supplementary Figure 1. Flow cytometry gating strategy of EC-derived ApoBD detection from plasma. Gating strategy used to detect population of EC-ApoBDs from mouse plasma using combined cell surface marker and cleaved caspase 3 staining. EC-ApoBDs were defined as $CD45^{-}$ / $CD11b^{-}$ /$CD41^{-}$ / FSC^{low} / $CD146^{+}$ / $CD31^{+}$ / $FLICA^{high}$ events. Analysis was performed using FlowJo Software (v10.8.2).

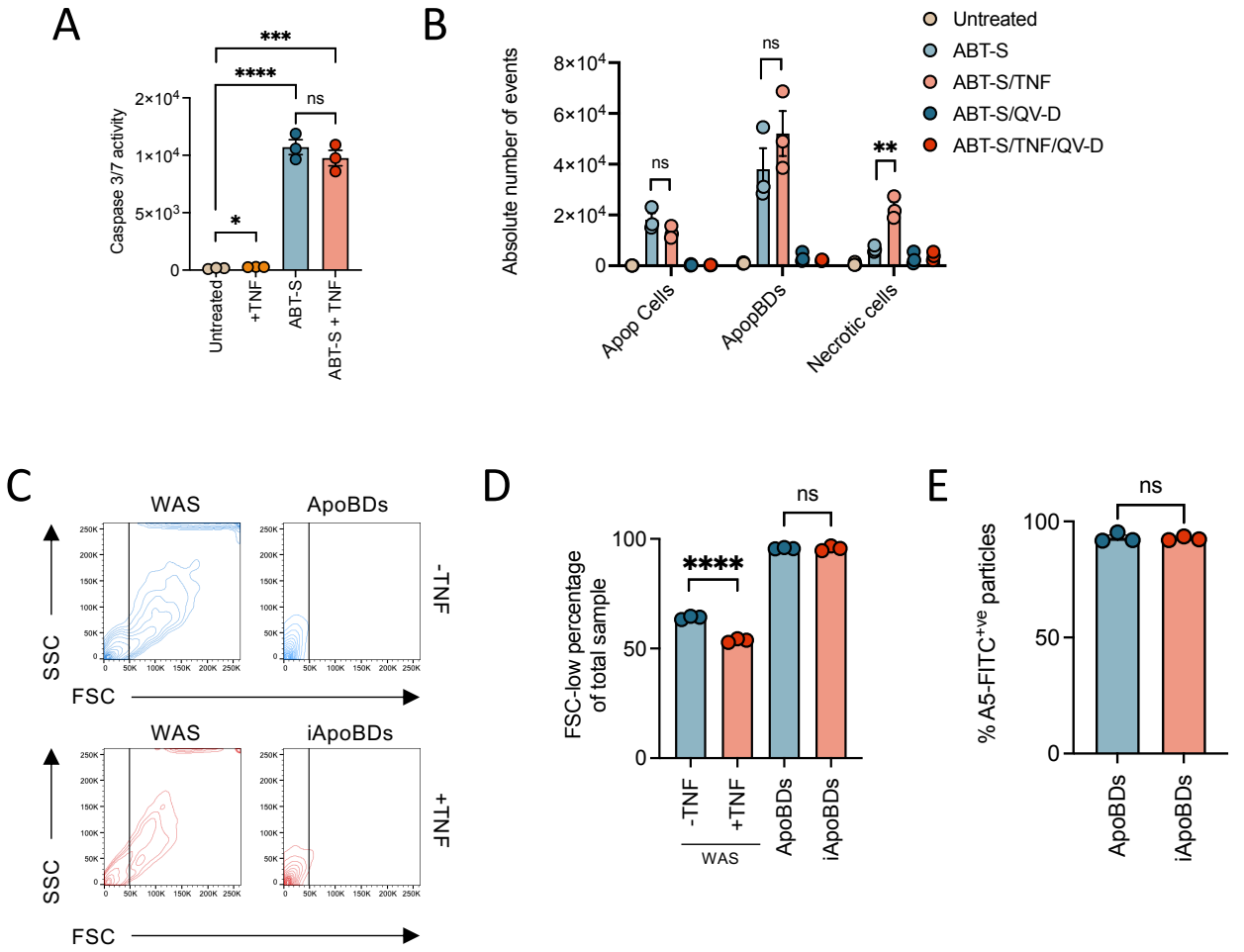

Supplementary Figure 2. Analysis of ApoBD generation, isolation and purity from human aortic endothelial cells (HAECs). (A) Level of caspase 3/7 activity in ABT-S-treated HAECs ± TNF (50 ng/mL), determined via Caspase-Glo 3/7 Assay. (**B**) HAECs treated with ABT-S to induce apoptosis ± TNF (50 ng/mL) were subject to flow cytometry analysis. Samples were stained with A5-FITC and TO-PRO-3 to identify necrotic cell, apoptotic cell and ApoBD populations. **(C)** Representative flow cytometry plots demonstrating enrichment of HAEC-derived small (FSC^{low}) particles in 'whole apoptotic sample (WAS)' compared to ApoBD-enriched samples following isolation protocol. Data is representative of three independent experiments. **(D)** Quantification FSC^{low} particles from (C). (**E**) Percentage of PtdSer-positive particles in ApoBD-rich samples following ApoBD isolation protocol, determined by A5-FITC staining. Error bars represent mean ± S.E.M. (n=3). P-values were determined using unpaired student's two tailed *t*-test, ns= not significant, ** = P<0.01, *** = P<0.001, *** = P<0.0001.

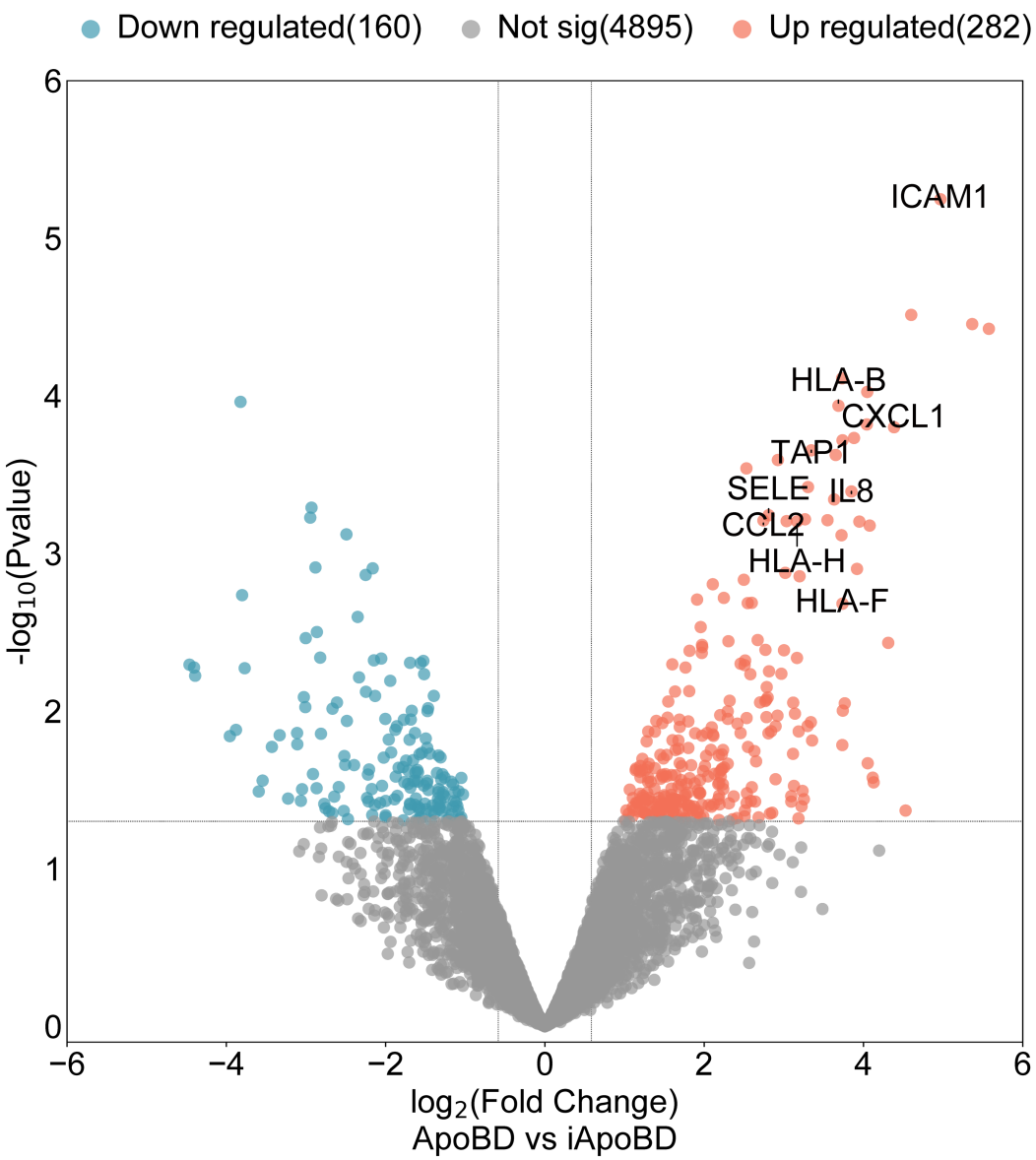

Supplementary Figure 3. Volcano plot displaying proteins enriched in iApoBDs. Volcano plot based on non-biased proteomics analysis comparing lysates from iApoBDs and ApoBDs. 282 proteins were upregulated and 160 proteins downregulated in iApoBDs based on a p-value cutoff of 0.05. Upregulated genes of interest annotated, n=3. Generated in SRplot.

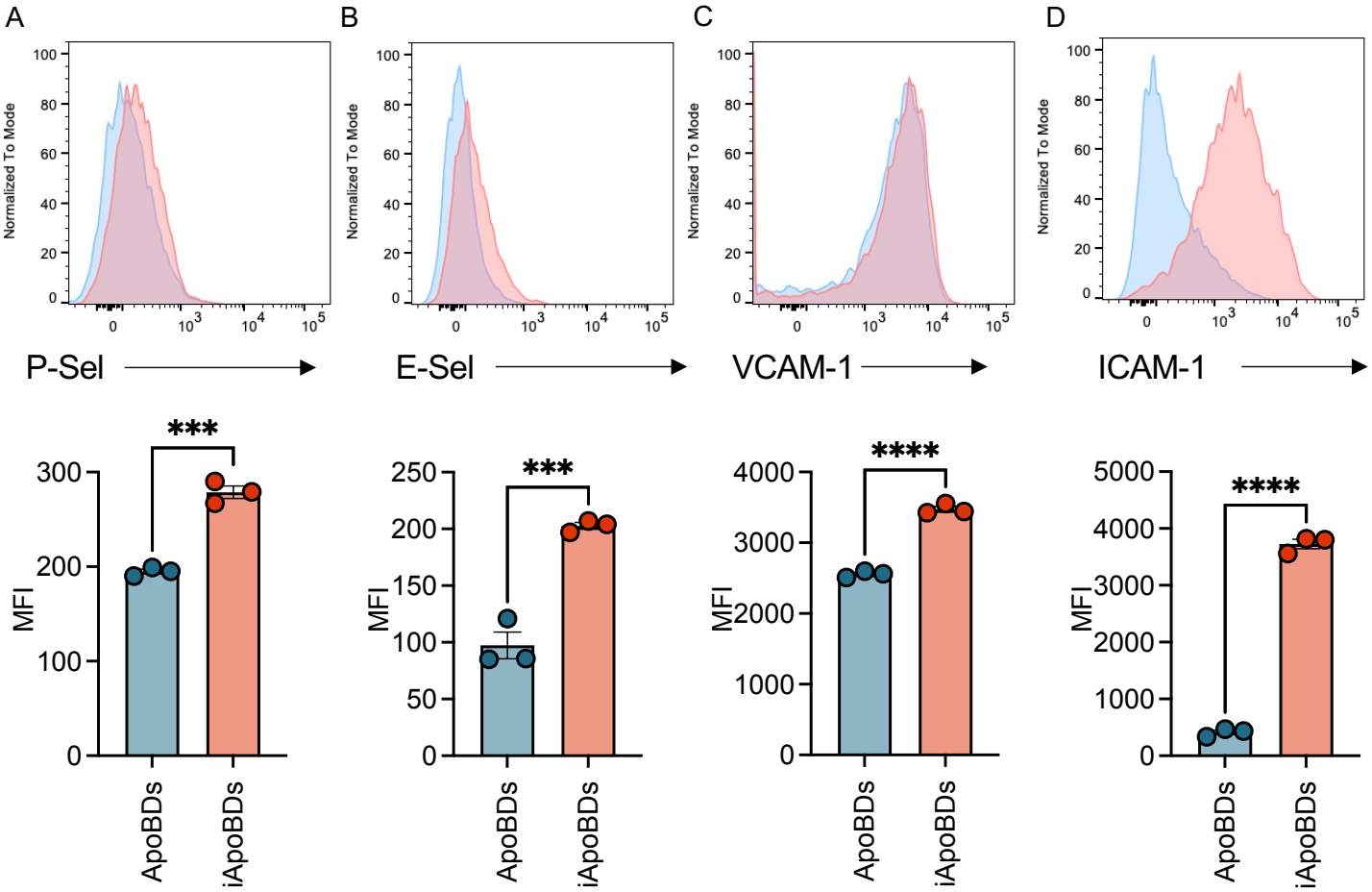

Supplementary Figure 4. HAEC-derived iApoBDs display enhanced expression of adhesion molecules. Surface expression of adhesion molecules P-selectin (A), E-selectin (B), VCAM-1 (C) and ICAM-1 (D) on HAEC-derived ApoBDs vs iApoBDs, determined by flow cytometry-based immunofluorescence. Upper: histogram shift in mean fluorescence intensity (MFI); Lower: quantification in bar graphs. Data represent three independent experiments. Error bars represent mean ± S.E.M., P-values were determined using unpaired student's two tailed *t*-test, *** = P<0.001, **** = P<0.0001.

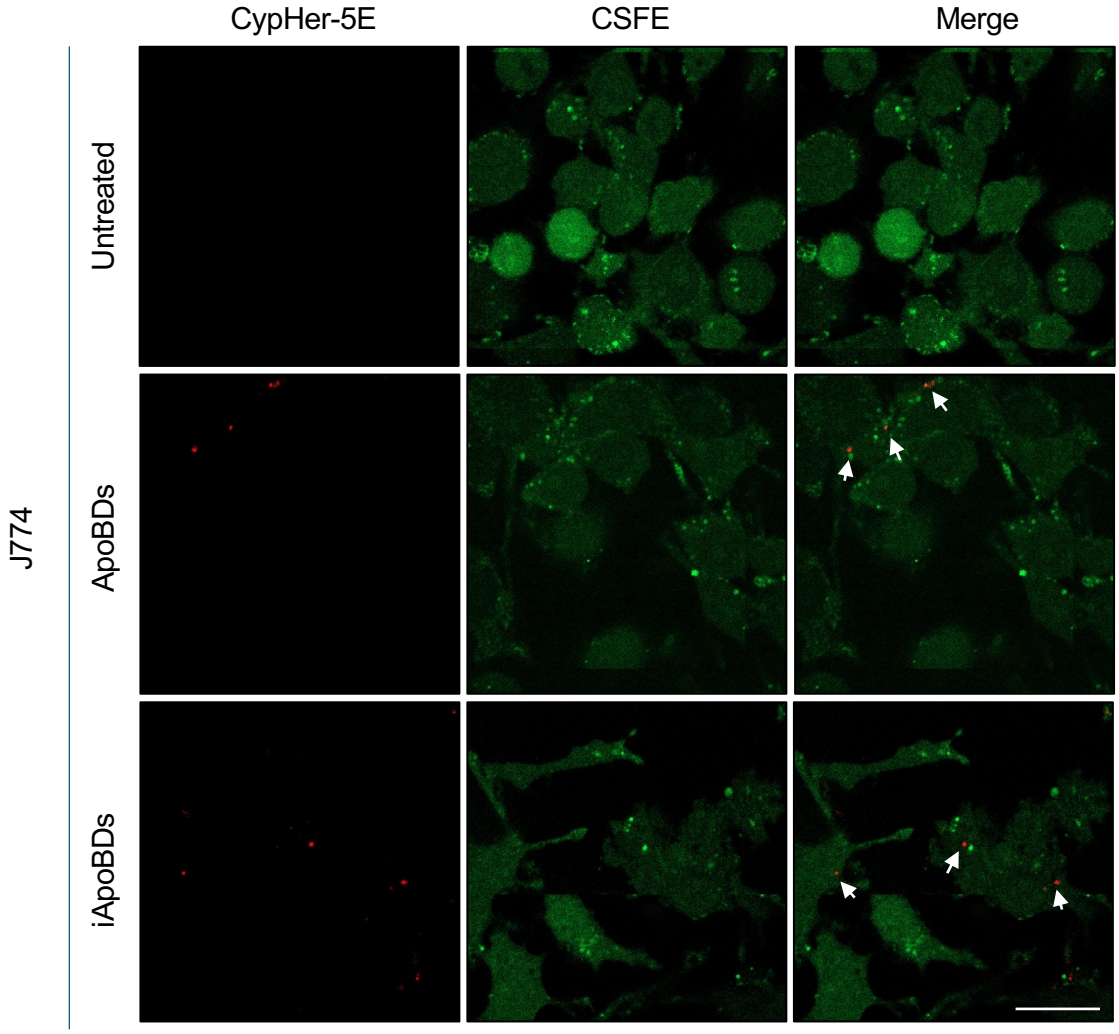

Supplementary Figure 5. Engulfment of EC-derived ApoBDs by J774 macrophages. Representative micrographs of J774 macrophages co-incubated with HUVEC-derived ApoBDs or iApoBDs. Data are representative of three independent experiments in which 5 x 5 tile regions were recorded per experiment at 63x magnification. Imaged using a LSM900 confocal laser scanning microscopy. White arrows indicate internalized CypHer5E+ apoptotic particles. Scale bar = 20µm.

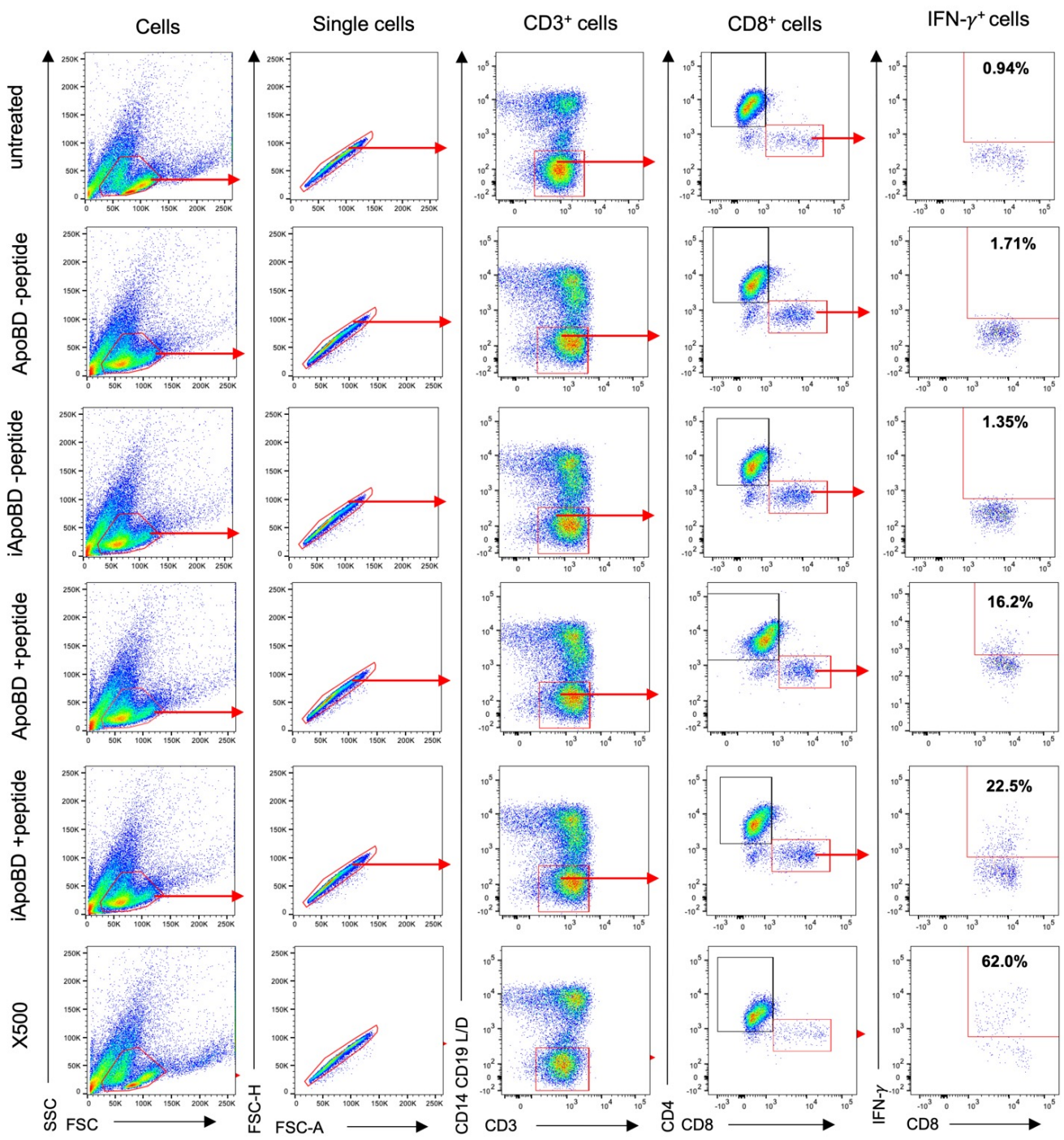

Supplementary Figure 6. Flow cytometry gating strategy for IFN-γ activation of T-cells. Representative gating strategy of human T cell lines activated through SARS-CoV-2 antigen presentation by ApoBDs from peptide pulsed HUVECs in Figure 5D-E.

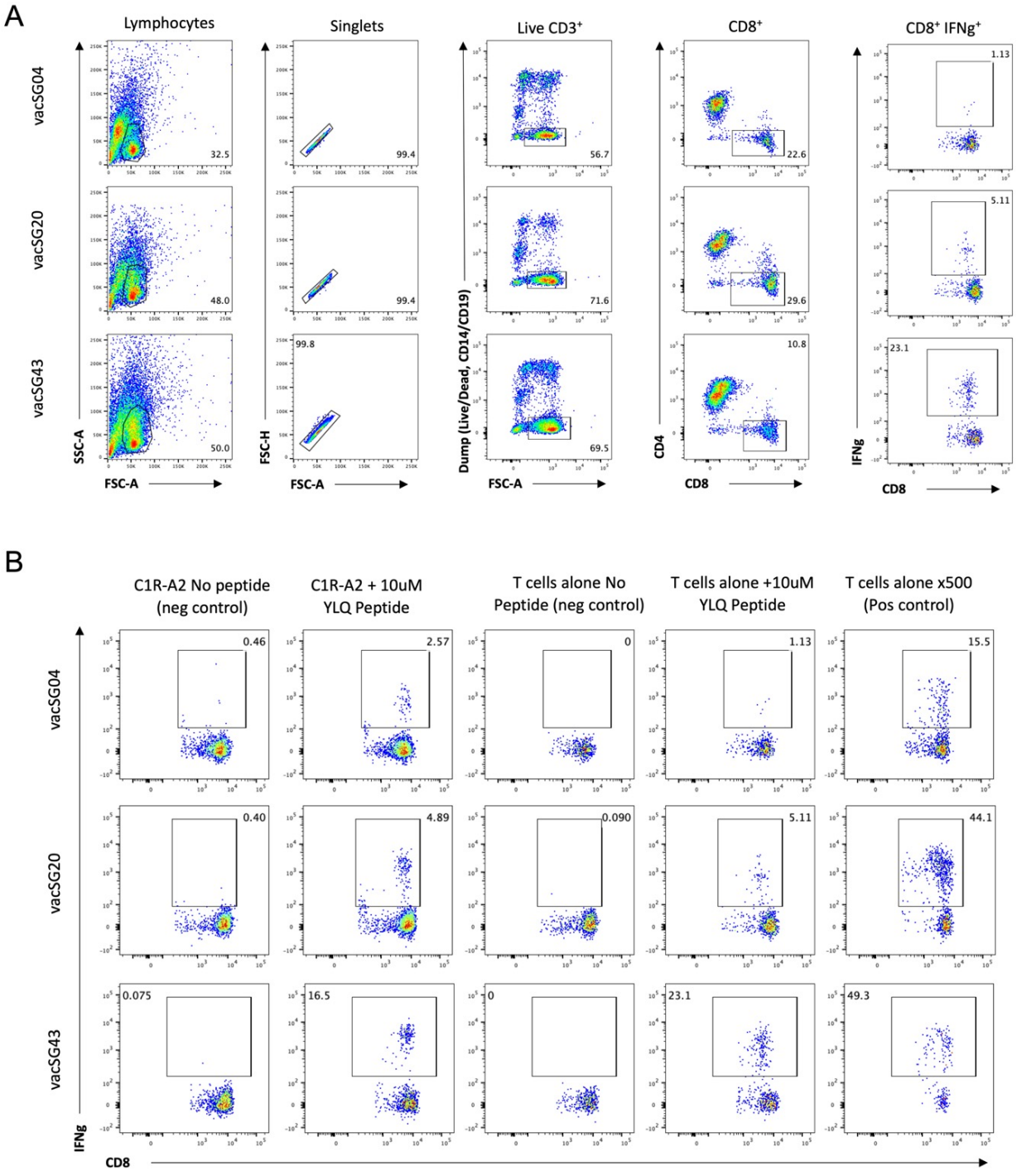

Supplementary Figure 7. Flow cytometry gating strategy of intracellular cytokine staining assay as a baseline of T-cell activation. PBMCs from HLA-A*02:01^{+} individuals were stimulated with 10 µM of the YLQ peptide to generate peptide-specific CD8^{+} T cell lines. CD8^{+} T cell responses were assessed using an ICS assay with or without antigen presenting cell lines. **(A)** Gating strategy used to assess IFN-γ production as a readout of CD8^{+} T cell activation. **(B)** CD8^{+} IFN-γ^{+} T cell responses towards the YLQ peptide, no peptide control or X500 positive control.